

DESIGN AND INTEGRATION OF AN ALL-MAGNETIC ATTITUDE CONTROL SYSTEM FOR FASTSAT-HSV01'S MULTIPLE POINTING OBJECTIVES

Brandon DeKock,¹ Devon Sanders,² Tannen Vanzwieten³, and Pedro Capó-Lugo⁴

The FASTSAT-HSV01 spacecraft is a microsatellite with magnetic torque rods as its sole attitude control actuator. FASTSAT's multiple payloads and mission functions require the Attitude Control System (ACS) to maintain Local Vertical Local Horizontal (LVLH)-referenced attitudes without spin-stabilization, while the pointing errors for some attitudes be significantly smaller than the previous best-demonstrated for this type of control system. The mission requires the ACS to hold multiple stable, unstable, and non-equilibrium attitudes, as well as eject a 3U CubeSat from an onboard P-POD and recover from the ensuing tumble. This paper describes the Attitude Control System, the reasons for design choices, how the ACS integrates with the rest of the spacecraft, and gives recommendations for potential future applications of the work.

INTRODUCTION

FASTSAT-HSV01 (FASTSAT) is a risk-tolerant microsatellite that launched into the designed 72 degree inclination, 650 km altitude orbit, on November 20, 2010. FASTSAT is the first in a family of spacecraft intended to be produced on a very rapid schedule for a modest budget. The spacecraft was designed as a collaborative effort between NASA Marshall Space Flight Center, Dynetics, the University of Alabama at Huntsville, and several other industry partners in Huntsville, Alabama. FASTSAT carries six payloads, three of which are upper atmospheric science experiments built by NASA Goddard Space Flight Center, and the other three are technology demonstration articles sponsored by the Air Force Research Laboratory. FASTSAT was built to NASA's Class D quality standards, which is the lowest quality grade for flight hardware, and this level of standards was appropriate due to the mission's risk tolerance, aggressive schedule, and small budget.

The design effort began in January 2009 and the assembly of the spacecraft was completed in September of 2009. The assembly had to be completed by this date to ensure a spot on the Air

¹ Guidance, Navigation, and Control Lead, Space Engineering Technology Division, bdSystems, an SAIC Company, Huntsville, Alabama

² Aerospace Engineer, Controls Systems Design & Analysis, NASA Marshall Space Flight Center, EV41, MSFC, AL.35812

³ Aerospace Engineer, Guidance, Navigation, and Mission Analysis, NASA Marshall Space Flight Center, EV41, MSFC, AL.35812

⁴ Aerospace Engineer, Controls Systems Design & Analysis, NASA Marshall Space Flight Center, EV41, MSFC, AL.35812

Force Space Test Program's S-26 Launch. Meeting this aggressive schedule was enabled by the use of pre-existing flight hardware which had been developed or purchased for a previously cancelled program. This already-chosen hardware suite included the magnetic torque rods, sun sensors, magnetometer, solar panels, battery, GPS receiver, and flight computer.

There are three features that make FASTSAT's Attitude Control System noteworthy among all-magnetic, non-spinning attitude control systems. The first is the pointing accuracy, which for some of FASTSAT's attitudes is intended to be up to an order of magnitude better than the previous best-demonstrated LVLH-relative all-magnetic attitude control. This is made possible using a periodic asymptotic Linear Quadratic Regulator (LQR) controller¹ and on-orbit characterization of the magnetic properties using measurements of the spacecraft dynamics. The second is that the ADCS will allow for several different LVLH-referenced attitudes, most of which are located at a gyroscopic or gravity-gradient instability. The third noteworthy feature is the ability to point a particular body vector toward a location on the ground as the satellite passes over the location. This allows an onboard sensor to observe a ground location, which is a task usually undertaken by satellites with much more complex attitude control systems.

SPACECRAFT LAYOUT AND FRAMES

The sides of FASTSAT are approximately 30 inches tall. A photograph showing the side with the P-POD and Star Tracker is shown in Figure 1. As suggested by the picture, the four vertical sides of FASTSAT are covered with solar panels, except for a portion of one of the sides with the P-POD door and Star Tracker. The nadir deck houses the remaining experiments, but it also has one solar panel. The launch-ring side of the bus, which is opposite the nadir deck, also has one solar panel inside the ring. Finally, there are three mutually orthogonal magnetic torque rods inside FASTSAT.

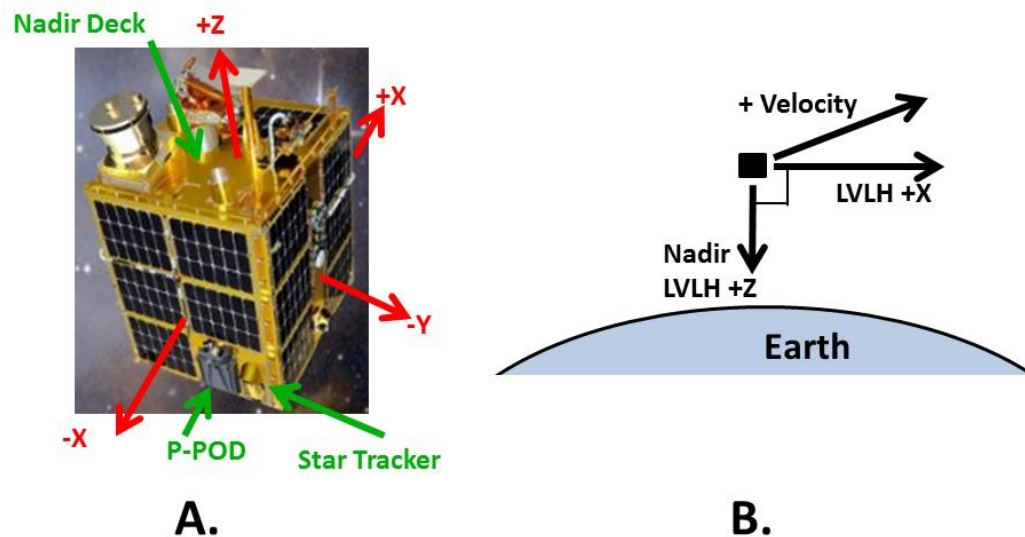


Figure 1. A. Picture of FASTSAT-HSV01 with reference coordinate system and component labels. B. Depiction of the LVLH reference frame convention used in this work.

The spacecraft body axes and a reference LVLH frame are depicted in Figure 1. These two coordinate frames are nominally aligned in one of the attitude modes, and the satellite also utilizes several other nominal attitudes. One of the attitudes has the satellite -Y axis aligned with the LVLH +X axis while the nadir deck remains nadir. Another LVLH attitude mode uses a

rotation about the LVLH Z axis of either of the two previously-described attitudes by an arbitrary angle. Another attitude points the spacecraft +Z axis toward the orbit-normal (LVLH-Y) and the spacecraft -X axis toward zenith (LVLH -Z).

The terms yaw, pitch, and roll are used to describe attitude rotations or perturbations relative to the LVLH axes and not the spacecraft body axes. There are two reasons for this. First, there are multiple nominal LVLH-relative orientations. Second, the available torque reactions are easier to conceptualize in the LVLH frame than in the body frame. For example, it is possible to generate a torque relatively close to the LVLH pitch axis, which is the LVLH Y axis, at any time in the orbit since the geomagnetic field vector is nearly perpendicular to the LVLH pitch axis the entire orbit. Using the same heuristic, the magnetic field is nearly parallel to the LVLH roll axis, which is the LVLH X axis, in the mid-latitudes. The magnetic field is also nearly parallel to the LVLH yaw axis, which is the LVLH Z axis, near the magnetic poles. Thus near these regions where the magnetic field is nearly parallel to a given LVLH axis, very little magnetic torque reaction is available about that axis.

ADCS HARDWARE

The ADCS hardware consists of four types of sensors and one type of actuator to perform the attitude determination and control functions of the spacecraft. The four sensors consist of a GPS receiver, a magnetometer, two sun sensors groups, and a star tracker. A Novatel GPS receiver is used as the spacecraft's time reference and provides position and velocity measurements for onboard and ground-based orbit estimation. A magnetometer built by Billingsley provides measurements of the local geomagnetic field. The two sun sensor groups are manufactured by Comtech AeroAstro and each group consists of five analog sun sensors. The groups are mounted on opposite sides of the spacecraft, providing nearly full spherical coverage. The star tracker is a Comtech AeroAstro Miniature Star Tracker, and this is the first flight of this star tracker model. Finally, the sole actuators for the ADCS are three magnetic torque rods. These torque rods were designed and built by the ES division at MSFC for a previous un-flown mission. The torque rods are mounted as a mutually-orthogonal triad aligned along the spacecraft body axes inside FASTSAT.

ADCS DESIGN CONSTRAINTS

Constraints Due to Schedule and Budget

The primary constraints on the design of the Attitude Determination and Control System (ADCS) were the tight schedule and low budget and the combination of these constraints influenced the design in various ways. These constraints affected hardware selection, software accuracy, software verification, and ADCS integrated testing.

The most significant effect of the schedule and budget was the requirement that the ADCS utilize the existing hardware from an earlier project. This meant all of the ADCS sensors and actuators, except for the star tracker, were already specified and procured prior to the design effort. In addition to influencing the hardware, the short schedule restricted the procurement of more accurate sensors and actuators. Reaction wheels would have been a more standard choice to meet the pointing requirements; however vendors were not able to deliver flight hardware within the short length of time available before assembly. Rate gyros were also not included in the design for the same reason as the reaction wheels.

The hardware inherited from the previous mission is not optimal for performance on this mission. The magnetic torque rods were oversized by a factor of 8 for this mission, which caused them to hold very large residual magnetic biases. It was necessary to change the degaussing

profile in the Magnetic Torquer Drivers to reduce this residual to a more acceptable level. Also, the sun sensor groups could not be installed on this satellite without being subject to glint from the solar panels and the sides of the bus. This is expected to degrade the accuracy of the sun sensors. Lastly, the battery from the previous mission was made of Ni-Cd cells, which have iron as a principal constituent. The residual magnetic dipole of the battery was characterized and found to be potentially significant, but not sufficient to saturate the actuators.

Due to the short amount of time available to design the integration strategy and the software, the ADCS team chose to sacrifice some accuracy of the onboard attitude and orbit determination algorithms in an effort to reduce the complexity and computational burden of the flight code, and to reduce the amount of testing necessary. Reducing the amount of time necessary to implement and test the algorithms was paramount, as the ADCS team was very small and the schedule was very aggressive. Two of the simplifications in the onboard algorithms were not using True of Date reference frames for attitude, and ignoring that the Star Tracker and GPS were asynchronous to the ADCS 1 Hz execution clock. The accuracy sacrificed was quantified and found to not significantly impact operations on-orbit, but necessitated logging onboard measurements for downlink and high-accuracy post-processing on the ground. This was deemed a good solution because ground-based post-processing software can be modified with much less substantial verification efforts than flight software. As with the attitude solution, a high-accuracy orbit determination solution is computed on the ground using downlinked GPS data.

Finally, the ADCS algorithm design and software testing process was accelerated through the use of autocoding through MatLab Simulink. The autocoding is discussed in more detail in the ADCS Integration section. Integrated testing of the ADCS on FASTSAT was also accelerated due to the required schedule. To enable the accelerated integrated testing, a large amount of parameterization was used inside the flight code to allow changing of the behavior of many aspects of the ADCS during testing and also later during on-orbit operations. This allows the software to be optimized to a large degree without requiring a code change after software verification. Substantial adjustability in the behavior of the flight algorithms through the use of parameters was deemed beneficial as it allowed for some robustness to unanticipated behavior.

Constraints Due to All-Magnetic Control

The sole attitude control actuators on FASTSAT are three magnetic torque rods, which limits the available control torques at any instant to the plane normal to the local geomagnetic field. As previously detailed, the pointing needs of the experiments dictated that the spacecraft hold various LVLH attitudes through most of the mission, which precluded spin-stabilizing the spacecraft. The implemented LVLH controller is the one described in Reference 1, with some minor modifications and an extension. This controller is an asymptotic periodic Linear Quadratic Regulator (LQR) controller used to control the roughly periodic system defined by the spacecraft's immersion in the geomagnetic field.

Accurate characterization of the satellite's mass properties is very important with all-magnetic control. Mis-characterization of the mass properties will result in unmodeled gravity gradient and gyroscopic torques. Though small, these torques are significant because no reaction torque is available about some spacecraft axis at all times. For FASTSAT, if the satellite's principal axes are not well aligned with the LVLH axes, there can be significant induced gyroscopic and gravity-gradient torques.

Lastly, a somewhat non-standard safe mode had to be adopted. Typically, in safe mode a solar panel would be pointed at the sun and held there. This ADCS does not have that ability and a

different approach is used. The feasibility of other approaches is facilitated by FASTSAT having solar cells on all sides.

Constraint Due to Launch Vehicle

FASTSAT's launch vehicle dictated that FASTSAT follow the Experimental Small Payload Adapter (ESPA) configuration, which specifies maximal dimensions of the satellite. The shape of some of the payloads, coupled with payload interoperability requirements, drove the requirement that the ADCS hold the satellite with the axis of rotation along its intermediate axis of inertia during some periods, a condition which is gyroscopically unstable.

The definition of the ESPA standard effectively limited the solar-power gathering area of FASTSAT, which uses only body-mounted solar panels. The limited area becomes important during times of low solar beta-angle, when eclipse length is at a maximum. In order to more effectively use the solar panel area during these periods, the ADCS holds FASTSAT in a gravity-gradient unstable attitude.

Payload Constraints on the ADCS

FASTSAT has six payloads, and accommodating all of their pointing needs is challenging. Alignment for the CubeSat ejection requires the ADCS to hold the satellite in a nominally stable attitude, with the principal axes nominally aligned with the LVLH axes. The ejection of the CubeSat nominally in the anti-velocity direction will impart a fast rotation (~ 7 degrees/sec) to FASTSAT, and the ADCS must then damp the rotation to continue with the mission.

A more challenging constraint is for the satellite to have the capability of pointing a sensor at a specific target on the ground as the spacecraft passes over the location. The innovative solution to this problem involves leaving the satellite in a gravity-gradient stable attitude while then holding any arbitrary yaw angle. Since any yaw offset angles that are not multiples of $\pi/2$ will cause gyroscopic disturbance torques, in the general case this attitude will be perturbed constantly.

Constraints Due to Having an Inertia Tensor that Changes Significantly

The ejection of the CubeSat will cause the minimum principal axis of the satellite to shift by six degrees. Attempting to point the minimum principal axis more than two degrees from nadir in the pitch direction induces oscillations about the yaw axis. When the pitch offset approaches seven degrees, these oscillations drive the attitude unstable and can cause the spacecraft to tumble. This is significant because two of FASTSAT's instruments are designed to operate with a precise offset from nadir, and as such, need to have the spacecraft Z axis (which is perpendicular to the nadir deck) within one degree of nadir. These circumstances combined dictate FASTSAT can only support these instruments fully either before CubeSat ejection or after ejection. Therefore, it was determined the CubeSat ejection should precede the operation of these instruments.

Constraint due to having a single-string system

Almost all of the satellite's systems are single-string. Since the satellite was built to NASA's Class-D quality standard, which is NASA's lowest quality rating for flight hardware, it is desirable to put failure tolerance into the software wherever easily achievable. The only instance of this in the ADCS code is in allowing for the uplink and propagation of a state vector in the case of a GPS failure. This enhancement was deemed worthwhile since the satellite's attitude control law requires knowledge of the current LVLH frame in order to function and because attitude determination requires an ECEF position vector to use the onboard geomagnetic field model.

ADCS INTEGRATION

Mass Properties

FASTSAT's pointing missions require the control of the alignment of the principal axes and an accurate characterization of the inertia tensor in order to minimize unmodeled torques. The ratios of FASTSAT's principal inertias after CubeSat ejection are $\sigma_1 = 0.34$, $\sigma_2 = -0.24$, and $\sigma_3 = -0.11$, where $\sigma_i = (I_{jj} - I_{kk})/I_{ii}$ for the (i,j,k) index sets (1,2,3), (2,3,1), and (3,1,2) as defined in Reference 1, with (1,2,3) corresponding to the principal axes near FASTSAT's (X,Y,Z) axes. The principal axes must be controlled because the non-axisymmetric mass properties create sizeable disturbance torques for FASTSAT if the principal axes are not aligned in the desired direction. Two of the experiments have requirements for their sensor boresights to be offset from nadir by a specific amount. Simulations showed the attitude controller could not reliably hold the minimum principal axis more than a few degrees off nadir, depending on gain matrix selection. Thus it was determined the minimum principal axis must be controlled to within 1.5 degrees of the spacecraft Z axis. This orients the spacecraft's nadir deck nominally orthogonal to within 1.5 degrees of nadir.

The orientation of the maximum and intermediate principal axes (the principal axes close to the Y and X body axes, respectively) about the minimum principal axis are not as constrained as is the orientation of the minimum principal axis. This is due to the near axis-symmetry between these two principal inertias. This allows for the minimization of the gyroscopic disturbance torques experienced when the ADCS holds an attitude where the principal axes are not aligned with the LVLH axes. It also reduces the severity of the gyroscopic instability when the satellite holds the attitude with the intermediate principal axis pointing parallel to the orbit normal vector.

The mass properties of FASTSAT were designed and controlled in a serial fashion throughout the very rapid design cycle. FASTSAT had significant mass margin available and this was used to allow the mechanical designers to create, and nearly finalize part designs for manufacturing without iterating component placement to tune the mass properties. Then the CAD-estimated mass properties were modified by both the addition of somewhat large internal brass masses and by the elimination of some of the material removal cuts from the aluminum structure in strategic locations. The design modifications were approved by the structural analyst, and then the components were manufactured. This approach essentially used mass margin to eliminate time-consuming iterations, thereby reducing design time, which was of primary importance.

It was necessary to obtain an estimate of the satellite's mass properties, whose inaccuracy was allowed to be no greater than the uncertainty allowed in the specification of the actual mass properties. To achieve this, the mass properties were measured after the satellite assembly was completed since the accuracy of the CAD model's mass property estimates was not believed to be sufficient. Due to mass-property measurement machine availability and scheduling constraints, the chosen method of determining the mass properties was somewhat non-standard. The chosen method was to use an available Moment of Inertia (MOI)-only machine and to make six MOI measurements about the appropriate axes along with CG and mass measurements. This information was then used to calculate the satellite's MOI's and Products of Inertia (POI's) using the POI-through-MOI method³. This method uses Mohr's Circle and the signed angles between MOI measurement vectors to estimate the POI's.

After the as-built mass properties were determined, it was found necessary to slightly adjust the lateral center of gravity for the launch vehicle tip-off in the CubeSat-stowed configuration, as well as adjust the minimum principal axis for after CubeSat ejection. This was accomplished by sizing trim masses and then attaching them to three of the eight external corners of the satellite.

The potential need to adjust the mass properties after the measurement was accommodated by the design and each of the eight external corners was built to allow the addition of a trim mass. The installation of the trim masses concluded the pre-launch mass properties design, characterization, and modification.

After FASTSAT has been on orbit for a brief period and as commissioning is nearing completion, two more events will occur that are significant to the mass properties. The first is the 3U CubeSat will be ejected from the P-POD and the P-POD door will remain open. The second event is as the satellite gradually slows from the resulting 7 degree/second tumble, the magnetic torquers will be turned off for periods to allow the observation of the un-forced dynamics using the star tracker and other sensors. Since the magnitude of the gyroscopic torques increase as the square of the body angular rates and the magnetic torques do not change with the body angular rates, this will provide the clearest opportunity to observe the gyroscopic torques, as they are magnified relative to the magnetic torques. These measurements will be used in an Extended Kalman Filter to provide more insight into the mass properties, especially the orientation of the principal axes.

Power

The ADCS interacts with the power system in two ways in addition to consuming power for the ADCS components. The battery has an uncompensated current loop that causes some dipole change when changing the battery's charge or discharge rate. The maximum magnitude of the dipole change between the maximum anticipated charge and discharge rates is $0.05 \text{ A}\cdot\text{m}^2$, which with nominal controller gains creates pointing errors up to 4 degrees. This disturbance is compensated for by providing the controller the battery current measurement as well as the vector-area of the current loop in the battery. This allows the controller to cancel the changing dipole and eliminate the disturbance torque.

The other coupling between the ADCS and the Power System is that the ADCS controls the pointing of the sides of the spacecraft, which contain the solar cells. In certain conditions, it is necessary for the ADCS to hold an attitude significantly different from all the others to ensure sufficient power generation. More detail is given in the section regarding the High Power-Generation Attitude.

Thermal and Communications

The Thermal Control and Communications systems did not place additional demands on the ADCS. The Communications system accommodates the nature of the ADCS by supporting high data rates when FASTSAT is able to point the antenna toward nadir, as well as a low data rate when pointing is severely degraded, such as during the de-tumble from the CubeSat ejection.

C&DH and Software Integration and Test

The aggressive schedule necessitated a streamlined process for generating the ADCS Flight Software. The method chosen was to use MATLAB Simulink as the algorithm design environment, and then to use MATLAB's Realtime Workshop Embedded Coder to generate the flight ADCS code. Using autocoding was deemed necessary very early in the design process due to the required development schedule; there was not time or manpower to generate a full Algorithm Description Document typically used to serially code, test, debug, and iterate between the ADCS group and the Flight Software group. This also allowed for streamlining the testing of the ADCS. The algorithms were designed, simulated, and unit-tested in MATLAB Simulink 2009A environment. Then a sub-set of these tests were re-run on an auto-coded and compiled version of the flight algorithms on the flight computer running the flight operating system. This was done by replaying a file of inputs that had been recorded in the Simulink environment. The

output from the flight computing environment was logged and compared to the outputs from the Simulink environment. The largest differences were at the level of machine precision, and thus it was determined that the autocoding and compiling had produced the desired result.

Integrated testing on the spacecraft had to be streamlined as well. This testing focused mostly on the interfaces to the flight ADCS algorithms since the algorithms themselves and the translation from Simulink to the flight environment had already been tested. The integrated testing started by verifying that sensor inputs and commands were received correctly and that the actuators were responding to commands as expected. Then orbit determination and attitude determination were tested using real or simulated inputs into all of the flight sensors, with the exception of the star tracker. The last step was an end-to-end test of orbit determination, attitude determination, and attitude control. For this test, the real GPS signal was used to calculate the translational state, the magnetometer sensed the actual geomagnetic field, and the sun sensors were stimulated by a sun simulator, while various attitude commands were issued. The attitude and orbit solutions matched the expected values within tolerance, and the commands to the magnetic torquers were compared to the expected commands, and found to agree.

Magnetics Testing

In order to perform the ADCS mission with a high degree of confidence, it would be necessary to test the important magnetic components of the satellite functionally while taking multiple field measurements, and then to test the entire satellite in the same way after assembly is complete. The reason for this is any unknown dipole on the satellite, due to a residual dipole or a coupling among the torquers or between a torquer and another satellite component, creates an unmodeled and thus uncompensated torque. One method of reducing the attitude disturbance due to this torque is to use higher gains in the feedback control loop. This method requires highly-accurate attitude determination, as otherwise attitude estimation errors can drive the system unstable. Since FASTSAT lacks rate gyros and the onboard attitude determination solution is not expected to be highly-accurate, it was determined that the approach of using very high gains to counter disturbance torques should not be relied upon and that characterization of the magnetic properties would be necessary. However, the project's schedule and budget did not allow for a complete magnetic characterization at a spacecraft magnetics facility. Thus, a detailed characterization of the spacecraft residual dipole, the coupling between the torquers, the coupling of the torquers to the ferromagnetic battery, and other interactions could not be performed before launch. Since this testing was not an option, another method was created for estimating most of these same magnetic properties. This is discussed in more detail in the section on Ground Processing.

Characterizing the effectiveness of the torque rod degaussing was performed locally. This testing used a Billingsley tri-axial magnetometer positioned at a skewed angle near the end of a torquer in a magnetically quiet environment while a series of commands were sent to the Torque Rod Driver unit. The response curves for magnetometer voltage out versus magnetic torque current input were constructed for each of the three magnetometer channels, and these were found to be linear with the exception of the hysteresis of the torque rod. Then the torquers were commanded through a representative profile of commands with degaussing applied after the actuation of each command. The three magnetometer measurements were recorded between commands after the degaussing. In this fashion, the magnetometer provided three independent measurements of the residual dipole on the torque after each command. This allowed the identification of some minor changes to the degaussing profile which resulted in an order of magnitude reduction in the amount of deviation in the residual dipole on the torquer. These changes were then implemented in the flight Torque Rod Driver units.

ATTITUDE DETERMINATION

As mentioned previously, most of the attitude and orbit determination hardware had been already procured and was available from a previous project. The magnetometer was a very reliable model with low noise, using a high-quality in-house Analog-to-Digital converter. Unfortunately, the previously-purchased analog sun sensors could not be mounted without having reflections from the solar panels corrupt the measurements somewhat. Regardless of the sun vector degradation, the attitude determination accuracy available from the aforementioned hardware was insufficient for the needs of some of the science instruments, so a star tracker was added to increase the overall accuracy. The measurements from the three attitude sensors are combined in an attitude filter based on a Lefferts-Markley Extended Kalman Filter² that uses vector measurements and rate gyro measurements to estimate attitude and gyro bias. This six-state indirect filter provides both an attitude estimate and a rate estimate. Since FASTSAT does not have rate gyros, this filter was modified so the gyro bias estimate is added to the predicted change in angular rate of the satellite due to estimated gyroscopic, gravity-gradient, and magnetic torques. This angular rate is an estimate of the spacecraft body rates, and it is then fed back into the filter in the place of the gyro measurement. This allows the filter to estimate and track the spacecraft body angular rates very well, and this estimate speeds convergence and reduces measurement residuals of the attitude filter. The filter is run onboard the spacecraft at 1 Hz, along with the rest of the ADCS algorithms.

Since this Lefferts-Markley filter is designed to only accept vector measurements in body frame, the attitude quaternion from the star tracker is rotated into body coordinates and then transformed into the equivalent Direction Cosine Matrix (DCM). Then the columns of this DCM are applied as measurements one at a time, with the reference vectors simply being the ECI Cartesian axes.

ATTITUDE COMMANDING

The attitude commanding algorithm generates the desired ECI to Body frame quaternion and the desired body rate commands. The satellite has several distinct LVLH-relative attitudes that can be commanded, each referred to as a different attitude mode. Each of these modes is expressed as a constant LVLH to body quaternion. The ECI to LVLH quaternion is then rotated by this LVLH to body quaternion. When a change in the LVLH to body attitude is desired, the new command is issued as a step-change, without any smooth transition in the command. This was selected over using a smooth command generator because the settling times were comparable, FASTSAT is not expected to change attitude modes often, and the step change is simpler to implement and test. This also simplifies the creation of the body angular rate command. The angular rate command is the angular rate of the LVLH frame transformed into body coordinates using the current attitude estimate. This makes the rate command independent of the attitude command, as shown in Eq.(1), where ω_{cmd}^B is the commanded angular rate in body coordinates, D_{BI} is the transformation matrix from the inertial reference frame to body coordinates, and ω_{LVLH}^I is the angular rate of the LVLH frame relative to the inertial reference frame, expressed in the inertial reference frame.

$$\omega_{cmd}^B = D_{BI} \cdot \omega_{LVLH}^I \quad (1)$$

The attitude commanding is based around maintaining the principal axes of inertia pointed along the LVLH axes in most of the attitude modes. For each attitude mode, the commanding algorithm has a quaternion which represents the commanded LVLH-relative attitude of the

spacecraft principal coordinate system. For example, the fourth-element scalar quaternion command to align the principal axes nominally with the LVLH frame axes is simply $q_{LP} = [0,0,0,1]^T$, and the quaternion command corresponding to a 180 degree rotation about the yaw axis is $q_{LP} = [0,0,1,0]^T$. Generating the ECI to Body frame quaternion then requires quaternion multiplication by the ECI to LVLH quaternion as well as the Principal Coordinates to Body Coordinates quaternion, as in Eq. (2) and Eq.(3). In these expressions, q_{EP} is the quaternion from ECI to principal coordinates, q_{EL} is the quaternion from ECI to LVLH coordinates, q_{LP} is the quaternion from LVLH to principal coordinates, q_{EB} is the desired attitude command from ECI to body coordinates, and q_{PB} is the quaternion from principal coordinates to body coordinates.

$$q_{EP} = q_{EL} \otimes q_{LP} \quad (2)$$

$$q_{EB} = q_{EP} \otimes q_{PB} \quad (3)$$

Most of the LVLH to principal axes quaternions are made by sequencing various 90 degree rotations about the LVLH axes. This is done to align the commanded principal axes of inertia with the axes of the LVLH frame so there are not any gyroscopic or gravity-gradient torques acting on the spacecraft. Some attitude modes require the ability to command a rotation of arbitrary value about an LVLH axis. This is applied as another rotation to q_{LP} as in the fourth-element scalar quaternions in Eq. (4) and Eq. (5) where the angle θ is the desired offset angle.

$$q_{offset} = [0,0,\sin(\theta/2),\cos(\theta/2)]^T \quad (4)$$

$$q_{LP_final} = q_{LP_initial} \otimes q_{offset} \quad (5)$$

This formulation is used in the Ground Location Pointing mode, and generally results in a gyroscopic disturbance torque. Another offset used is about the LVLH pitch axis and is applied the same as above, moving the $\sin(\theta/2)$ term from third element of the quaternion to either the first or second element, depending on which body axis is commanded to be close to the LVLH pitch axis.

ATTITUDE CONTROL

The performance of the attitude controller was simulated extensively in a Simulink environment along with the rest of the ADCS algorithms, sensor models, and environment models in order to develop reasonable expectations of the on-orbit performance of the system. FASTSAT's main attitude controller is a nine-state asymptotic periodic LQR LVLH attitude controller, which is a modest extension of the one described by Psiaki (see Reference 1). The controller is mechanized in the best estimate of the spacecraft principal axis frame. The error quaternion between the attitude command and the attitude estimate is q_{err} , which is expressed with a non-negative scalar element. The computation of the error angles and integrated error angles is shown in Eq. (6) through Eq. (8), where θ_{EA} is the eigen-angle of the error quaternion, \hat{q} denotes the scalar element of a quaternion, \bar{q} is the unit-norm eigen-axis of a quaternion, and dt is the discrete timestep of the controller.

$$\theta_{EA} = 2 \cdot a \cos(\hat{q}_{err}) \quad (6)$$

$$\theta_{err} = \bar{q}_{err} \cdot \theta_{EA} \quad (7)$$

$$z_{i+1} = z_i + \theta_{err} \cdot dt \quad (8)$$

The integral errors are then state-limited to prevent them from becoming too large. The rate error is simply the commanded rate minus the estimated rate. Each of these three error vectors is then transformed from body frame to principal axis frame by multiplying by the DCM that rotates from body frame to principal axis frame. They are then concatenated into a 9x1 error vector with the ordering of the states matching the order of the states in Reference 1. The geomagnetic field measurement is then transformed from body frame into principal frame using the same process. The dipole command u in the principal frame is then computed in Eq. (9)

$$u = -R^{-1} * B(t) * P_{ss} * x_{err} \quad (9)$$

where R is a 3x3 identity matrix, $B(t)$ is the control effectiveness matrix described in equations 6,7, and 22a from Reference 1, P_{ss} is the steady-state gain matrix described later, and x_{err} is the error state vector.

The dipole command is checked for saturation (see Reference 1) of a soft-limit and then transformed back into body coordinates from principal coordinates. The estimated spacecraft residual magnetic bias is then subtracted from the dipole command. The Magnetic Torquer Drivers drive the torquers with a pulse of uniform length and allow the sign and magnitude of the current to be varied. The torquer pulse length is then compensated for by multiplying by the appropriate scalar gain. Then the torquer scale factor and cross-coupling are compensated for by multiplying the dipole command by the 3x3 torquer correction matrix in Eq. (10) :

$$u_{torquer} = G_{Corr} * u_{cmd} \quad (10)$$

where u_{cmd} is the commanded dipole vector in body coordinates, G_{Corr} is the non-orthogonal, non-normalized correction matrix, and $u_{torquer}$ are the dipole commands to be acted upon by the torquers. More is said about the correction matrix in the Ground Processing section. The commands to the torquers are then multiplied by the scalar conversion from dipole to milliAmps, and the command is sent to the torquers to be actuated at the next timestep.

The main difference between this implementation and that reported in Reference 1 is the elimination of the α_0 scaling parameter to increase the gains. There were two reasons for omitting this feature. First, FASTSAT's torquers were sufficiently large that saturation was not normally an issue. This allows the nominal gains to be somewhat higher than the slow gains given for the satellite described in Example 1 in Reference 1. Also, the upper bound of the expected attitude determination errors could possibly drive the system unstable if using gains for a high-bandwidth system. Other differences are the book-keeping of coordinate frames, duty-cycle correction, and the use of the torque correction matrix.

Disturbances:

Simulation of the attitude controller performance showed that some of the disturbance sources were negligible, while others were potentially very large and required substantial mitigation efforts. The planned launch date corresponds to a period approaching solar maximum, and for a 650 km altitude circular orbit, the solar pressure and dynamic pressure due to the expanded atmosphere are of similar magnitude. However the torques on FASTSAT due to either of these is small due to the spacecraft's shape and not having deployed solar arrays, resulting in the center of

mass being very close to the center of pressure. However an unknown onboard magnetic dipole will have a significant impact on the pointing accuracy. The torque correction matrix must also be formed correctly, or significant magnetic disturbance torques will result. These magnetic properties will not be measured prior to launch, and must be estimated once the satellite is on-orbit. The accuracy of the mass property estimate is equally important, but the expected accuracy obtained from the ground-based mass-property measurements is nearly sufficient for all of FASTSAT's pointing objectives. An on-orbit characterization of the mass properties is planned to ensure sufficient accuracy in the mass-property estimates.

Direct Commanding Mode: The simplest attitude mode for FASTSAT is to allow the direct commanding of each torquer individually. This mode is used to characterize the mass properties and the magnetics of the satellite and does not point any of the body axes in any particular direction. Typical use is a sequence of scheduled commands actuate the torquers one at a time at a constant level for several minutes, and allow for some times when no torquers are active. This is intended to provide observability of all of the magnetic states.

Safe Mode: The next simplest mode does not require a translational state estimate or attitude determination estimate, it simply requires a properly functioning magnetometer. FASTSAT's Safe Mode consists of calculating a B-dot damping command to damp rates and then superimposing on that a constant bias of $+2 \text{ Amp}\cdot\text{m}^2$ onto the Z-axis torque rod. The B-dot damping command is calculated by taking the discrete derivative of the magnetic field in body coordinates and then multiplying that by a scalar gain less than zero. The damping results in the nulling of rates relative to the geomagnetic field, and the bias ensures that after the rates have been nulled the nadir deck and fixed antenna will point roughly along the geomagnetic field line. At high northern latitudes, the geomagnetic field lines point somewhat close to nadir, which is desirable since FASTSAT's primary ground sites are at high northern latitudes. Safe Mode is also used for recovering from the 7 deg/sec spin caused by the ejection of the CubeSat.

LVLH Attitude Control Modes:

The ACS is designed to hold many distinct LVLH-relative attitudes. Since the LQR controller contains a linearization about a specific operating point, it is expected that the performance should degrade far from that operating point. This was observed in simulation, and as a result, each distinct attitude mode has a 9×9 gain matrix. The calculation of a gain matrix, referred to as the P_{ss} matrix or steady-state gain matrix since it is not time-varying and hence steady-state, is performed on the ground, and the method of doing this is explained in equations 20 and 21 in Reference 1. The notation from that reference is followed here. For all of the attitude modes described here, the R matrix was simply the identity matrix. Values for the diagonal Q matrices are given below with the description of each attitude mode. The values of the Q matrices were determined using manual tuning of the parameters.

LVLH Capture and Hold: This mode seeks to align the nadir deck with nadir and the maximum principal axis with either the orbit normal or opposite the orbit normal. This is a gravity-gradient stable attitude and also a gyroscopically stable attitude. This mode requires onboard translational navigation and attitude determination to have valid estimates. This is because the error quaternion used to drive the LQR controller is the error between the estimated LVLH frame and FASTSAT's estimated principal axis frame. This attitude control mode is essentially the one described in Reference 1, with the exception of the gain-scaling that is used if the errors are sufficiently small. The weights in the diagonal weighting matrix Q used for this attitude are $Q = \text{diag}(1 \times 10^{-8}, 1 \times 10^{-9}, 1 \times 10^{-9}, 2, 0.2, 0.2, 2, 0.2, 0.2)$. Using these gains in the spacecraft simulation resulted in attitude control errors of 1.5 degrees.

This attitude mode is used as an intermediate attitude between other modes since it is stable. It also can point the P-POD ejection vector close to the anti-velocity vector and is used for the ejection of the CubeSat.

Intermediate Axis Rotation: This attitude differs from the previous attitude by a rotation of 90 degrees about the nadir axis. The minimum principal axis still points nadir, however the intermediate principal axis points to the orbit normal or anti-orbit normal. This is gravity-gradient stable, but gyroscopically unstable. Similar to the LVLH Capture and Hold mode, orbit and attitude estimates must exist for the same reasons. This attitude requires an extension to the work presented in Reference 1 due to the change in the orientation of the satellite. The computation of the gains for this attitude is accomplished by calculating the gains for a satellite with the MOI ratios rearranged so that σ_1 and σ_2 are switched. Then it is seen that the resulting 9x9 steady-state gain matrix is actually nine 3x3 matrices. Each of these 3x3 matrices is then rotated from the LVLH frame, which was used for the initial computation, to the satellite body frame in the intended attitude. This rotated 3x3 matrix is then placed back into its same location in the 9x9 P_{ss} gain matrix. This operation maintains the symmetry and positive definiteness of the steady-state gain matrix. This simple frame rotation is used in the calculation of all of the gain matrices, with the trivial case being the LVLH Capture and Hold gain matrix, where the rotation of the gain matrix is performed using identity DCM's. The rotation of one of the 3x3 submatrices of the 9x9 gain matrix is performed in Eq. (11) similarly to a frame rotation of an inertia tensor, and is shown in Eq. (12) where P_{3x3}^L is one of the 3x3 matrices from the 9x9 P_{ss} matrix which has been calculated in LVLH coordinates, D_{BL} is the DCM from LVLH to principal body coordinates and D_{LB} is its inverse, and P_{3x3}^B is the 3x3 gain matrix rotated into the nominal principal body frame.

$$P_{3x3}^B = D_{BL} \cdot P_{3x3}^L \cdot D_{LB} \quad (11)$$

This is valid when the D_{BL} rotation consists of any series of 90 degree rotations about the principal axes. However it was found to not result in useable gain matrices when used with rotations of arbitrary angles. The weights in the diagonal weighting matrix Q used for this attitude are $Q = \text{diag}(1 \times 10^{-9}, 1 \times 10^{-8}, 1 \times 10^{-9}, 0.2, 2, 0.2, 2, 0.2, 2)$. Using these gains in the spacecraft simulation resulted in attitude control errors of 1.5 degrees, equivalent to the performance in the gyroscopically stable attitude.

This attitude mode also needs to allow small angular offsets of +/- 4 degrees about the LVLH pitch axis. The gain matrix does not change for this, and the controller is fed the quaternion command with the pitch offset included. Achieving this pitch offset requires applying a nearly-constant torque about the pitch axis to counteract the gravity-gradient torque. The inclination of the orbit relative to the geomagnetic equator causes the pitch-axis torque to couple into yaw and roll axes, manifesting as a yaw oscillation whose amplitude is roughly twice the pitch axis offset. The frequency of the oscillation is nominally once per orbit, with the difference due to the rotation of the geomagnetic pole with the Earth. This yaw oscillation was not found to be useful for the expected operation of FASTSAT's experiments.

High Power-Generating Attitude: This attitude is potentially used during periods of low beta angle when FASTSAT will be in eclipse more than a third of the time. This attitude points the maximum principal axis in the +V direction and the minimum principal axis toward orbit normal. For FASTSAT's geometry and solar cell coverage, holding this attitude during times of low beta angle would maximize solar energy gathering. It is, however, gravity-gradient unstable about the LVLH roll (X) axis. The geomagnetic field is nearly parallel to the LVLH roll axis

around the mid-latitudes. This inability to torque in the direction of the instability for large portions of the orbit results in poor performance in holding this attitude in simulation. However, moderate attitude perturbations do not significantly degrade solar energy gathering compared to holding the attitude precisely. The simulated performance significantly enhances solar gathering over the baseline attitudes that have the nadir deck pointed nadir. The weights in the diagonal weighting matrix Q used for this attitude are $Q = \text{diag}(1 \times 10^{-10}, 1 \times 10^{-10}, 1 \times 10^{-11}, 2, 2, 0.2, 2, 2, 0.2)$.

Another gravity-gradient unstable attitude was investigated but not found useful for FASTSAT's mission. This attitude is a 90 degree rotation of the LVLH Capture and Hold attitude about the pitch axis. The performance in holding this attitude was far better than for the performance holding the High Power-Generation attitude. This is because in this case, the primary gravity-gradient instability is about the pitch axis, and reaction torque is available about this axis throughout the orbit. The instability for the High Power-Generating attitude is about the roll axis, and reaction torques are unavailable about this axis for much of the orbit. This was achieved using the same gain matrix as in the LVLH Capture and Hold without any rotations applied to the matrix itself.

Ground Location Pointing: This attitude mode is used to point the boresight of a sensor at a location on the surface of the Earth. Since there is insufficient control authority to keep an arbitrary body-fixed vector pointed near a point on the surface throughout a potential observation, a different method of control is used. The chosen method assumes the spacecraft cannot reliably hold a gravity-gradient unstable or non-equilibrium attitude. This means attempting to hold any non-zero LVLH-relative pitch or roll command is not feasible, and thus the minimum principal axis remains pointed nadir. This leaves the yaw angle about the minimum principal axis as the only degree of freedom. It was also determined the ADCS could not track a rapidly changing yaw command, and thus a constant yaw command must be chosen for each ground observation. This method requires that the sensor boresight vector be offset from the minimum principal axis. The greater the angle between these two, the greater the maximum cross-range viewing distance, as long as the boresight vector still intersects Earth. The geometry of an observation is shown below in Figure 2.

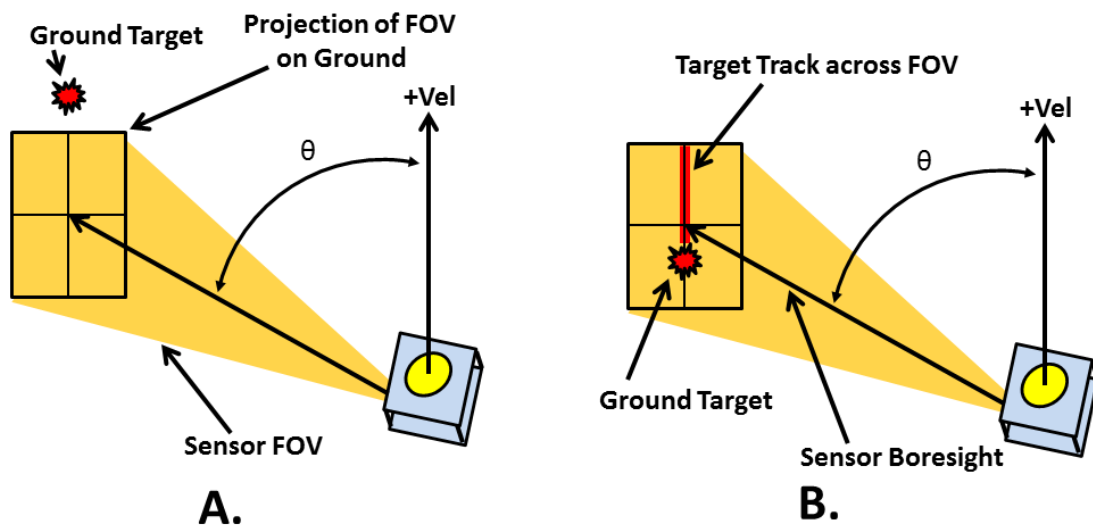


Figure 2. Overhead view of geometry for viewing a ground location observation. In A, note the angle θ is between the horizontal planar projections of the velocity vector and the boresight vector. In B, the track of the ground location across the sensor FOV is shown as a red line.

It is shown in Figure 2 that allowing the yaw angle to go between negative -90 and +90 degrees is sufficient to perform all possible observations when the ground location is within range. For the geometry in the figure, this observation will occur as the satellite is approaching the ground location. Additionally, allowing the yaw angle to take on any value between -180 and +180 degrees allows for a second opportunity for the measurement, as the satellite has passed the ground location and is retreating.

The gyroscopic disturbance torque generated by holding an arbitrary yaw angle is a function of the mass properties and the angle between the principal axes and the LVLH axes. If the LVLH attitude were perfectly held and the orbit were perfectly circular, the gyroscopic disturbance torque would be constant and solely about the yaw axis. The magnitude of the gyroscopic torque is maximal when the principal axes are 45 degrees from the LVLH axes, and the torque is zero when the two axes align. However, there is limited reaction capability about the LVLH yaw axis when the spacecraft is near the geomagnetic poles. This limitation allows the disturbance torque to become an attitude disturbance. The system's roll-yaw coupling then causes the attitude disturbance to transfer to the roll axis as well. The controller also reacts against these roll and yaw attitude disturbances, and in the process creates a small pitch disturbance due to the geomagnetic field not being perfectly orthogonal to the pitch axis, thereby allowing the coupling. The magnitude of the attitude disturbances due to this coupling was mitigated two ways. The first method was to install internal masses to make the mass properties more axis-symmetric. The next was to manually tune the Q matrices used to generate the gain matrix.

It is not feasible to successfully perform both the approaching and retreating observations for one overhead pass since the settling time for slewing to a new attitude ranges from five to eight orbits, while the maximum possible time between the advancing and retreating observation opportunities is less than 20 minutes for this orbit. The method used to determine which candidate is preferable analyzes both candidate observations and determines whether the star tracker boresight passes near enough to the sun to cause a measurement outage immediately prior to, or during, the observation. If this yields no preference, then both candidate observations undergo a dispersion analysis, with the track of the ground location across the sensor Field of View (FOV) recorded for each dispersed run. One of the dispersed variables is the time of the command to slew to the observation attitude, as the time of this command was found to significantly affect the settling time. This analysis results in a dispersed set of streaks across the sensor FOV, which are nearly parallel. The mean of the set of FOV tracks is then calculated by averaging the points where the tracks intersect the boundary of the FOV at the point of entry into the FOV as well as for the exit point. Due to the previously mentioned attitude oscillations, this mean track across the FOV is unlikely to cross the boresight of the FOV. The angular offset and direction to the closest approach between the boresight and the mean FOV track is then used to calculate a slightly different initial yaw command, and the analysis is re-run with that modified yaw command. The standard deviation of the width of the dispersed FOV tracks is then calculated and stored. The analysis is then repeated for the other candidate observation attempt, and the observation with the lower standard deviation is selected as the best candidate. The standard deviations of the track widths are expected to be different due to the different attitudes causing gyroscopic torques with opposite signs and different magnitudes.

It was noticed that re-tuning the Q matrix weightings could result in a modest reduction in the roll and yaw oscillations when holding an attitude with the maximal gyroscopic disturbance, a 45-degree yaw offset. To take advantage of this reduction in perturbations, the onboard control

system has eight P_{ss} matrices used with this mode. The P_{ss} matrix used is the one that was tuned and coordinatized to work in the sector where the yaw angle was commanded. Each gain matrix then has a 45-degree yaw sector within which it is considered valid. Note that the gain matrices themselves are not rotated by 45 degrees, as this is invalid.

GROUND PROCESSING

Due to limited onboard computing resources and limited schedule to design and test flight algorithms, the high-accuracy attitude determination for the ADCS is done on the ground as post-processing. GPS measurements are logged onboard and downlinked to allow for high-accuracy orbit determination and prediction using a non-linear Least-Squares batch filter. Star tracker measurements, attitude estimates, commands to the torquers, and magnetometer measurements are logged and downlinked to enable Kalman smoothing of the attitude estimate. The torque commands are logged to provide knowledge of the torques applied to the spacecraft, allowing more accurate attitude estimation.

An Extended Kalman Filter (EKF) is used to estimate a refinement of the mass properties and the magnetic characteristics of FASTSAT. This filter uses the orbit estimate, the smoothed attitude estimate, and the commands to the torquers to estimate the spacecraft mass properties and the magnetic properties of the spacecraft and the torquers. Mass property estimation is done using the measurements taken during the slowing of the tumble caused by ejecting the CubeSat. The body rates are at their peak, causing the gyroscopic torques to be at their peak value also. The magnetic properties are characterized by commanding the torquers through a pre-defined sequence that provides observability into the alignment and gain of the effective dipole of each torquer. The command sequence also has some periods where all three torquers are commanded to zero current so that there is observability of the residual magnetic bias on the spacecraft itself.

The mass property estimates and the spacecraft magnetic state estimates calculated using this EKF are included in parameter updates that are the uplinked to the FASTSAT ADCS onboard software. This is necessary because the controller uses these parameters in calculating the commands to the torquers. To the degree that these parameter estimates are wrong, unmodeled torques are applied to the satellite, resulting in attitude perturbations. The torquer effectiveness matrix, along with the torquer correction matrix which is used in the controller, are defined in Eq. (12) and Eq. (13) where M_{true} is the actual dipole generated by the torquers, G_{Eff} is the torque effectiveness matrix, u_{cmd} is the commanded dipole, and G_{Corr} is the torque correction matrix used onboard.

$$M_{true} = G_{Eff} * u_{cmd} \quad (12)$$

$$G_{Corr} = [G_{Eff}]^{-1} \quad (13)$$

The off-diagonal elements in G_{Eff} correspond to coupling between the torquers or to other satellite components which create an off-axis dipole when a torque is activated. The diagonal elements are simply scale factors on each of the three torquers. This model assumes that all of the materials are able to respond linearly to the magnitude and direction of the aggregate magnetic field.

RECOMMENDATIONS AND FUTURE APPLICATIONS

Recommendations

All-magnetic attitude control has many drawbacks, mostly resulting from the inability to apply torque about the local geomagnetic field vector. Magnetic dipoles on the spacecraft are constantly changing due to electrical currents in power system wires, and residual magnetization of the spacecraft itself can vary with time and orientation in the geomagnetic field as well. Since these changing dipoles create disturbance torques, it is necessary to estimate and compensate for the dipoles or to have high gains in the attitude controller.

Accurately measuring a magnetic dipole on a geometrically complex object is not a simple undertaking. This is exacerbated if the geometrically complex object has time-varying electric currents inside it, such as those moving through a power system or through magnetic torquers. As mentioned previously, obtaining estimates of these properties before launch can be a substantial undertaking, which likely becomes more substantial as the satellite gets larger.

Before choosing all-magnetic attitude control for a satellite, the designer should understand the mission-specific design space of pointing requirements, performance risk, desired reliability and satellite lifetime, desired performance flexibility, cost, and satellite size. All-magnetic attitude control can be highly reliable on long missions, as there are no moving parts or tanks to deplete, however the pointing requirements must be achievable. Reaction wheels or thrusters allow large amounts of flexibility in pointing compared to magnetic torque rods, which are relatively limited in the number of attitudes that can be held. For a satellite in the Microsatellite class, the cost of doing a full magnetic and mass property characterization, which may be necessary to prove ADCS robustness and reduce performance risk, may be commensurate with the cost to use small reaction wheels. In this case the better solution may be to use reaction wheels or thrusters, due to the increased flexibility. However for a CubeSat, more performance risk may be acceptable and miniature reaction wheels too costly or power-hungry, in which case all-magnetic control may be attractive. Magnetic characterization of a CubeSat is likely less expensive than characterization of a larger satellite due to the relative ease of transportation to a suitable test facility⁴ and the greater availability of smaller test facilities.

If all-magnetic attitude control is selected, it is recommended that the actuators be properly sized to the mission. For some satellites, air-core torquers may be appropriate, otherwise degaussing may be necessary. Also, it is advisable to provide provision for estimating and correcting for magnetic biases, misalignments, and scale factors. If this calibration information is to be gathered with the satellite on-orbit, accurate attitude determination information will be necessary.

Future Applications

This controller could potentially be used in a nanosatellite platform, such as a CubeSat, to allow it to point payloads at specific ground targets. The shape of a 3U CubeSat lends itself readily to this type of magnetically actuated pointing, as the gyroscopic torques due to the difference between the maximum and intermediate principal inertias are very small, and the gravity gradient torques which act to assist in the stabilization are relatively large.

Another application of this ACS could be on very long-duration missions that require LVLH attitude control. Since this ACS does not have moving parts or consume propellant, it is theoretically not life-limited. An actual satellite embarking on a long-duration mission in Low Earth Orbit, however, would have a C&DH system subject to radiation hazards as well as power system degradation. The power system would also need to be tolerant to periods of tumbling and solar off-pointing.

A theoretical advancement that would aid with both of these future applications would be computationally efficient and reliable parameter estimation of the magnetic residuals and couplings, as well as the mass properties, which could be run continuously onboard the satellite. This has the potential to reduce or eliminate the need for performing these characterizations on the ground, thereby saving significantly on cost and schedule.

SUMMARY

FASTSAT-HSV01 is a risk-tolerant microsatellite that was designed and built on a very short schedule. The short schedule dictated that already-available magnetic torque rods be the only actuators. The pointing requirements driven by the science payloads dictated that the pointing accuracy be significantly better than the previous best-demonstrated for LVLH-relative all-magnetic attitude control.

The mission requires the satellite hold various LVLH-referenced attitudes, and the asymptotic periodic LQR controller described in Reference 1 was extended to allow for holding multiple distinct attitudes. Also, it was discovered that a yaw oscillation occurs due to a commanded small pitch-axis offset.

The most notable contribution of this work is the method for pointing a sensor at a ground location while leaving the satellite in a gravity gradient-stable attitude and commanding a slew solely about the yaw axis. Targeted ground location observations are typically reserved for satellites with more capable attitude control systems.

The compressed schedule drove many aspects of the ADCS design, integration, and testing plan. Aside from using magnetic torque rods to achieve a very demanding pointing mission, the torque rods themselves are oversized, and the sun sensors had to be mounted in a manner that subjected them to reflections from the spacecraft body. The onboard algorithms were simplified as much as possible to reduce design time and algorithm testing time. Time-consuming iteration of internal component placement to control the mass properties was eliminated by allowing large and small trim masses to be sized and added later in the design process. Schedule and budget constraints precluded testing to characterize the spacecraft magnetics properties in a spacecraft magnetics facility. Since the information gained from this characterization is essential, this will be performed after launch using ground-based post-processing of the attitude dynamics measurements taken during maneuvers designed to make these magnetic states observable.

ACKNOWLEDGEMENTS

The authors would like to thank the NASA Marshall Space Flight Center, the Von Braun Center for Science & Innovation, Dynetics Inc., and the Air Force Space Test Program for making this work possible. The authors would also like to thank Don Hediger, Bill Rooker, Tom Bryan, and John Rakoczy for their contributions to the Attitude Determination and Control System.

REFERENCES

¹ M.L. Psiaki, "Magnetic Torquer Attitude Control via Asymptotic Periodic Linear Quadratic Regulation." AIAA Guidance, Navigation, and Control Conference, Denver, CO, August 2000, AIAA-2000-4043.

² J.L. Crassidis, J.L. Junkins, *Optimal Estimation of Dynamic Systems*, Chapman and Hall / CRC, 2004, pp 419-430.

³ W. Middelael, B. Rathbun, K. Wiener, "A Step by Step Procedure for Determining Product of Inertia Using the Moment of Inertia Method." 68th Annual SAWE Conference, Wichita, KS, May 2009, SAWE Paper 3476.

⁴ J.C. Springmann, J.W. Cutler, H. Bahcivan, "Magnetic Sensor Calibration and Residual Dipole Characterization for Application to Nanosatellites." AIAA Guidance, Navigation, and Control Conference, Toronto, Ontario, CA, August 2010, AIAA-2010-7518.